Measuring Cell Adhesion Forces with the Atomic Force Microscope at the Molecular Level

Martin Benoit   Hermann E. Gaub

Center for Nano Science, Ludwigs-Maximilians-Universität, Munich, Germany

Abstract

In the past 25 years many techniques have been developed to characterize cell adhesion and to quantify adhesion forces. Atomic force microscopy (AFM) has been used to measure forces in the pico-newton range, an experimental technique known as force spectroscopy. We modified such an AFM to measure adhesion forces between live cells or between cells and surfaces. This strategy required functionalizing the surface of the sensors for immobilizing the cell. We used *Dictyostelium discoideum* cells which respond to starvation by surface expression of the adhesion molecule csA and consequent aggregation to measure the adhesion force of a single csA-csA bond. Relevant experimental parameters include the duration of contact between the interacting surfaces, the force against which this contact is maintained, the number and specificity of interacting adhesion molecules and the constituents of the medium in which the interaction occurs. This technology also permits the measurement of the viscoelastic properties of single cells or cell layers.

Copyright © 2002 S. Karger AG, Basel

Introduction

Cell adhesion has been investigated using many techniques. Light microscopy has been combined with antibody staining, GFP expression, shear flow [Kuo et al., 1997] and optical tweezers [Dai and Sheetz, 1995] to characterize the points of adhesion between cells. Electron microscopy provides high-resolution images of adhesion sites and underlying protein networks [Thie et al., 1995]. Protein expression studies allow examination of the molecular components appearing before, during and after the formation of adhesion contacts [Scott et al., 1995]. While such approaches have advanced our understanding of cell adhesion, they do not look at the force against which the adhesion is maintained. By means of

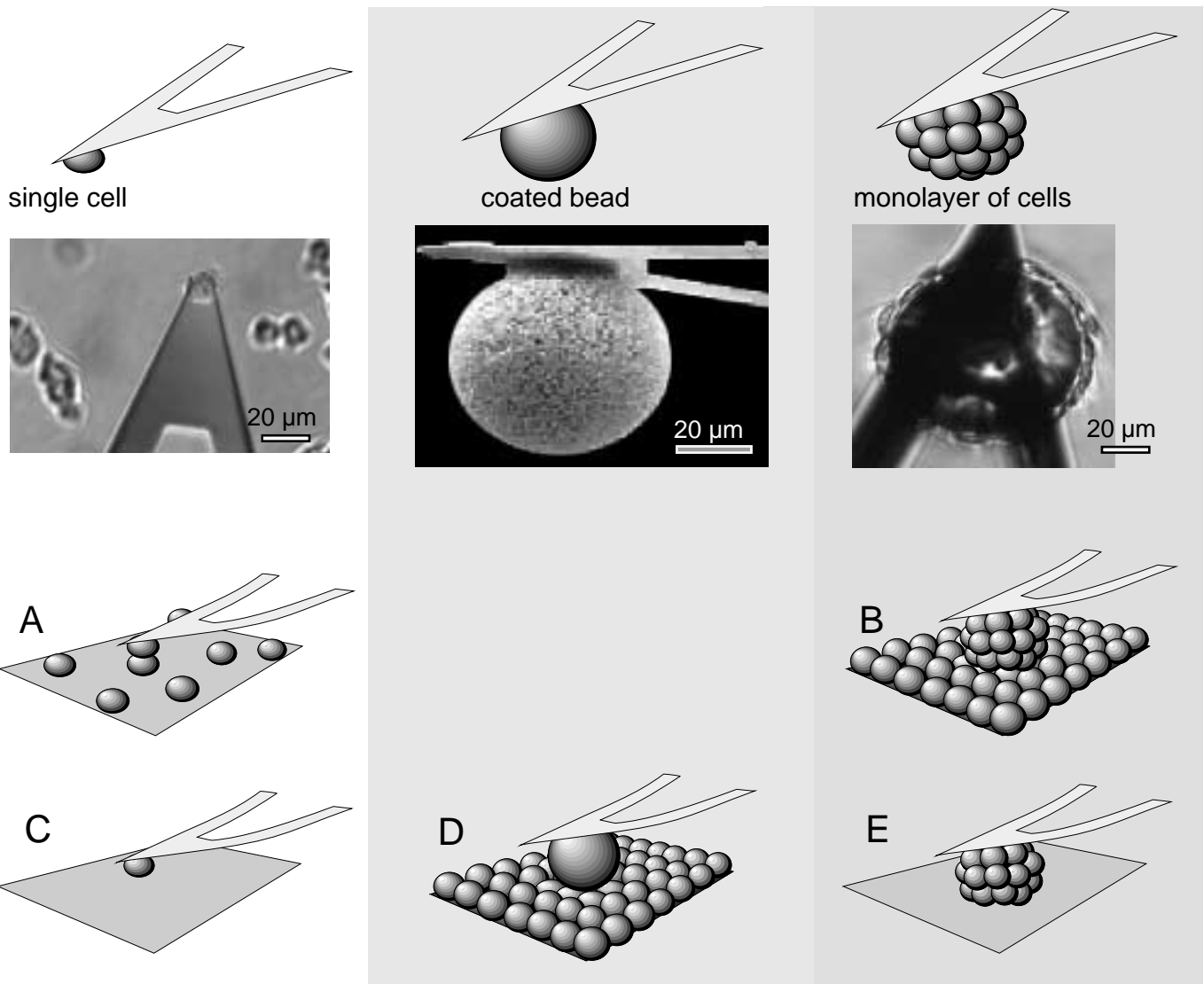| Abbreviations used in this paper	
AFM	atomic force microscope
ATCC	American Type Culture Collection
EDC	1-ethyl-3-(3-dimethylaminopropyl)carbodiimide
EDTA	ethylenediaminetetraacetic acid
FCS	fetal calf serum
HPL	*Helix pomatia* lectin
NHS	N-hydroxysuccinimide
WGA	wheat germ agglutinin

Fig. 1. Cartoon of three different possibilities of sensor modifications for cell adhesion measurements with images of modified sensors. Schematics below: Single cell interaction with a cell (**A**) and with a surface (**C**), interaction of a cell layer with a spherical surface (**D**) and a spherical layer with a plain surface (**E**), and cell layer interaction with a cell layer (**B**).

centrifugation assays [John et al., 1993], shear flow [Alon et al., 1995], cell poking [Zahalak et al., 1990] and micropipet [Evans et al., 1994] techniques the forces of adherent cells were determined. However, the interacting forces were not resolved at the molecular level, and this made distinguishing between many weak or few strong bonds impossible. In order to address this limitation, we have developed an atomic force microscope (AFM)-based assay which allows for direct measurement of the forces required to sever contacts between live cells (de-adhesion forces). Since AFM technology has already proven useful for stretching and unfolding individual molecules and for measuring bond strengths [Gaub and Fernandez, 1998; Clausen-Schaumann et al., 2000], it provides an ideal technique for characterizing mechanical contacts between cells down to the single molecule level.

To that end we immobilized cells on a substrate or on the force sensor itself. Cells immobilized on the sensor were then used to investigate cell-cell interaction (fig. 1).
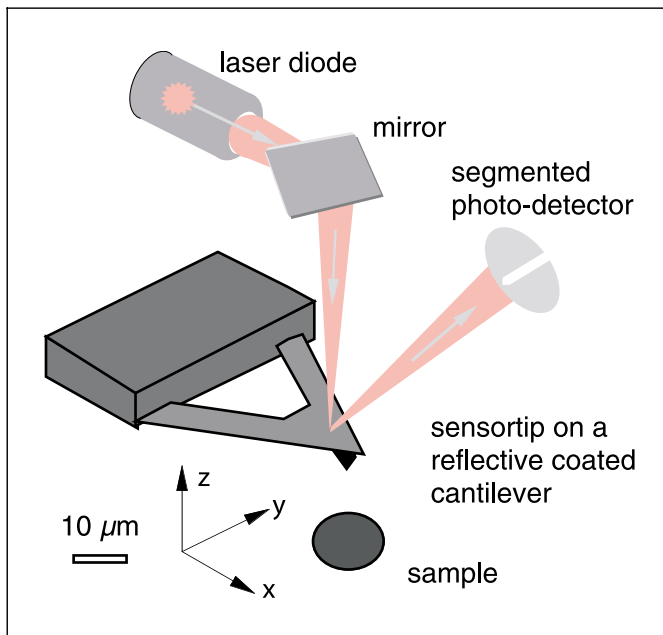
Fig. 2. Schematic illustration of the AFM technique; a laser beam is reflected from the cantilever into a segmented photodiode. The interaction forces of the tip with the piezo-positioned sample deflect the cantilever and thus displace the laser beam on the segmented detector.

We characterized complex cell layers with multiple interacting surfaces and likely myriad interacting moieties. In order to understand the basic principles of cell adhesion, we characterized a simpler system involving lectin-mediated adhesion between two otherwise nonadherent red blood cells [Grandbois et al., 2000]. Finally, we measured the forces between the calcium-independent adhesion molecules of csA that were expressed on the surfaces of *Dictyostelium discoideum* cells under starvation conditions [Benoit et al., 2000].

Materials and Methods

The Force Spectrometer
The AFM [Binnig et al., 1986] can be used to measure nano-newton to pico-newton forces and micrometer to ångström displacements. Such measurements utilize a microfabricated Si_3N_4 spring (cantilever), which interacts via a small tip with the sample. A diode-laser beam is focussed on the gold-coated surface of this sensor device (fig. 2) and reflected into a detector: the beam deflection thus measured provides a signature of cantilever deflection. Once the spring constant of the cantilever is determined, the displacement observed can be translated into force measurements. Except for those with sphere, where the spring constant was determined before mounting

the sphere, the spring constant of the cantilever in each experiment was determined using a thermal noise technique described earlier [Florin et al., 1995]. The instrument is mounted on an inverted optical microscope. A covering Perspex box and a heating stage are used to control the environmental conditions for cultured cells. The Petri dish with the cells could be moved along the microscope axis towards the sensor by a piezo-controlled positioning stage with a range of 100 µm (fig. 3).

The Force versus Distance Plot
A force versus distance curve represents a force experiment (as e.g. in fig. 5). The piezo displacement is plotted along the x-axis against the force calculated from the measured cantilever deflection on the y-axis. Negative forces indicate repulsion whereas positive forces reflect adhesion.

Sensor Preparation and Modification
To measure cell-cell adhesion, we modified both the sensor and the instrument. In order to achieve smooth surfaces for the cells to adhere to, the tip is either removed from the cantilever with tweezers (fig. 4) or a sphere is glued onto it. The sensor surfaces are functionalized with an adhesive molecule [Grandbois et al., 2000] to immobilize cells on the sensor without harming them. A non- or weakly adherent single cell is then fished from the bottom of the Petri dish (fig. 6) [Benoit et al., 2000], or alternatively cells are incubated on the sphere in order to grow a monolayer [Thie et al., 1998]. Figure 1 shows a summary of the possible modifications and their applications.

Surface Preparation
Aminosilanization
The Si-OH layer of a glass surface or of the standard commercially available Si_3N_4 cantilever (Microlever, Park Scientific Instruments) was silanized with N^1-[3-(trimethoxysilyl)propyl]diethylenetriamine (Aldrich) at 80°C for 10 min, washed in ethanol and cross-linked in water at 80°C for 10 min in order to obtain an amino-functionalized surface [Grandbois et al., 2000].

Surface Functionalization with Carboxy Groups
Aminosilanized surfaces were either inactivated or prefunctionalized by incubation in a PBS (Sigma) solution (pH 7.4) of 10 mg/ml of activated carboxymethylamylose (Sigma). The carboxymethylamylose was activated with 5–10 mg/ml N-hydroxysuccinimide (NHS, Aldrich) and 2–10 mg/ml 1-ethyl-3-(3-dimethylaminopropyl)carbodiimide (EDC, Sigma) for 5 min, and the surfaces were then rinsed 3 times in PBS [Grandbois et al., 2000].

Covalent Protein Attachment
Freshly carboxymethylized surfaces (after 10 min incubation time) are still activated by the EDC and NHS. An immediate wash in PBS and incubation in a 100–1,000 µg/ml protein solution [e.g. 0.5 mg/ml wheat germ agglutinin (WGA); Sigma] in PBS (pH 7.4) for 2 h will covalently link free NH_2 groups of the protein to the remaining activated carboxy groups of the carboxyamylose. Intensive rinsing in PBS removed unbound protein [Dettmann et al., 2000].

Metallized Glass Slides
Titanium (Ti, Goodfellow), titanium-vanadium (TiV, Goodfellow) and cobalt-chromium (CoCr, Goodfellow) were thermally evaporated at room temperature in vacuum (10^{-5} Pa) onto cleaned glass coverslides to a thickness of about 50 nm [Domke et al., 2000].

Fig. 3. Sketched setup of the cell-adhesion-force spectrometer; the sensor-laser-detector unit is placed from above into the Petri dish on the piezo stage. From below the microscope objective makes it possible to watch the cells during the experiments. Cell culture conditions are obtained by covering the instrument with a CO_2 chamber with a heating stage.
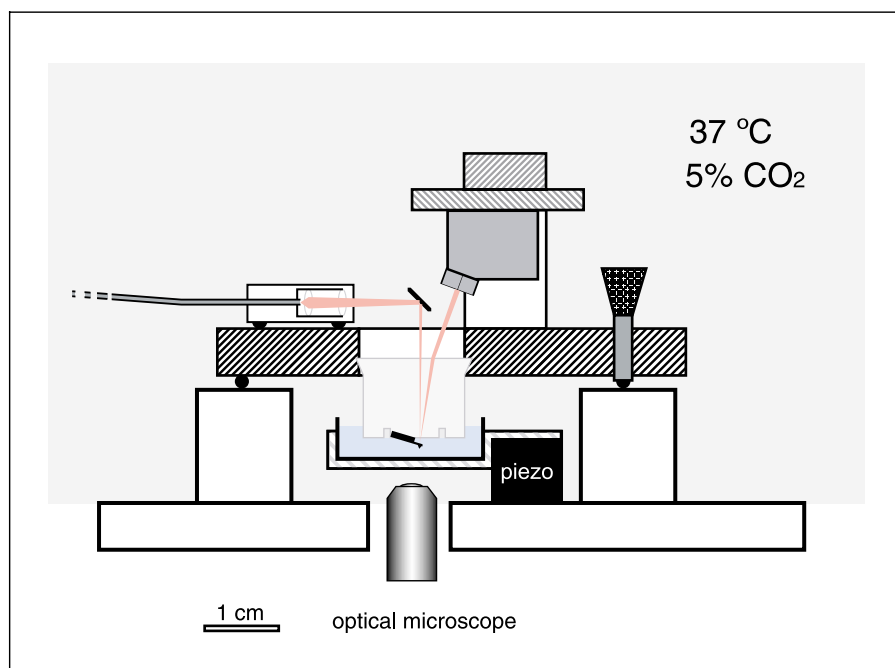
Cell Culture

SaOS$_2$ Cell Culture on Cantilever

Cantilevers mounted with Sephacryl microspheres as described above were immersed in 0.01% poly-D-lysine for 1 h at room temperature, washed 3 times in SaOS$_2$ medium: MEM/F12 medium (Gibco) supplemented with 3,080 mg/l HEPES (Sigma), 1.2 g/l NaHCO$_3$ (Gibco), 100 ml/l fetal calf serum (FCS; Gibco), 20 ml/l penicillin-streptomyocin (Gibco), 20 ml/l MEM vitamins (Gibco) and 12 ml/l amphotericin B (Gibco). pH is adjusted to 7.4. These are then subsequently incubated with an SaOS$_2$ [American Type Culture Collection (ATCC), Manassas, Va., USA] cell immersion (200,000 cells/ml) in SaOS$_2$ medium. After the SaOS$_2$ cells had settled, these cantilever-cell combinations were incubated in 5% CO_2-95% air at 37°C. Usually within 3–4 days after the start of the cultures, the cells had spread to a confluent monolayer over the sphere (fig. 5). We then used these spheres for experiments in either SaOS$_2$ medium or HBSS (Sigma).

HEC RL JAR Cell Culture on Coverslips [Thie et al., 1998]

Measurements on human endometrial cell lines, purchased from the ATCC (Rockville, Md., USA), i.e. HEC-1-A [short HEC; HTB 112; Kuramoto et al., 1972] and RL95-2 [short RL; CRL 1671; Way et al., 1983] were performed in JAR medium at 36°C and 5% CO_2. For routine culture, we grew cell lines in plastic flasks in 5% CO_2-95% air at 37°C. In brief, HEC cells were seeded out in McCoy's 5A medium (Gibco-Life Technology, Eggenstein, Germany) supplemented with 10% FCS (Gibco), RL cells in a 1 + 1 mixture of Dulbecco's modification of Eagle's medium and Ham's F12 (Gibco) supplemented with 10% FCS, 10 m*M* HEPES (Gibco) and 0.5 µg/ml insulin (Gibco). Human JAR choriocarcinoma cells [ATCC: HTB 144; Patillo et al., 1971] were cultured in RPMI 1640 medium (Gibco) supplemented with 10% FCS and 0.1% glutamine. All media were
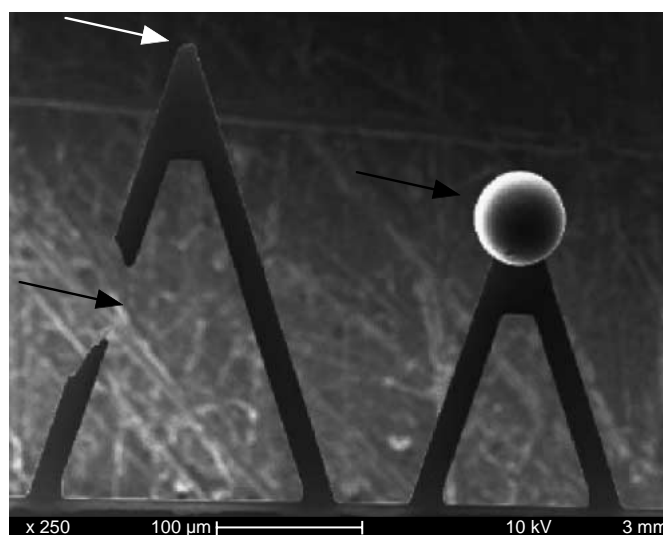

Fig. 4. REM image of the modified force sensors (cantilever). Arrows indicate the modifications: removed tip (white arrow) for immobilizing cells, broken leg for compliant sensors and mounted sphere on the smaller cantilever.

further supplemented with penicillin (100 IU/ml; Gibco) and streptomycin (100 µg/ml; Gibco). The growth medium was changed every 2–3 days, and cells were subcultured by trypsinization [trypsin-ethylenediaminetetraacetic acid (EDTA) solution; Gibco] when they became confluent. Cells used in experiments were harvested by trypsin-
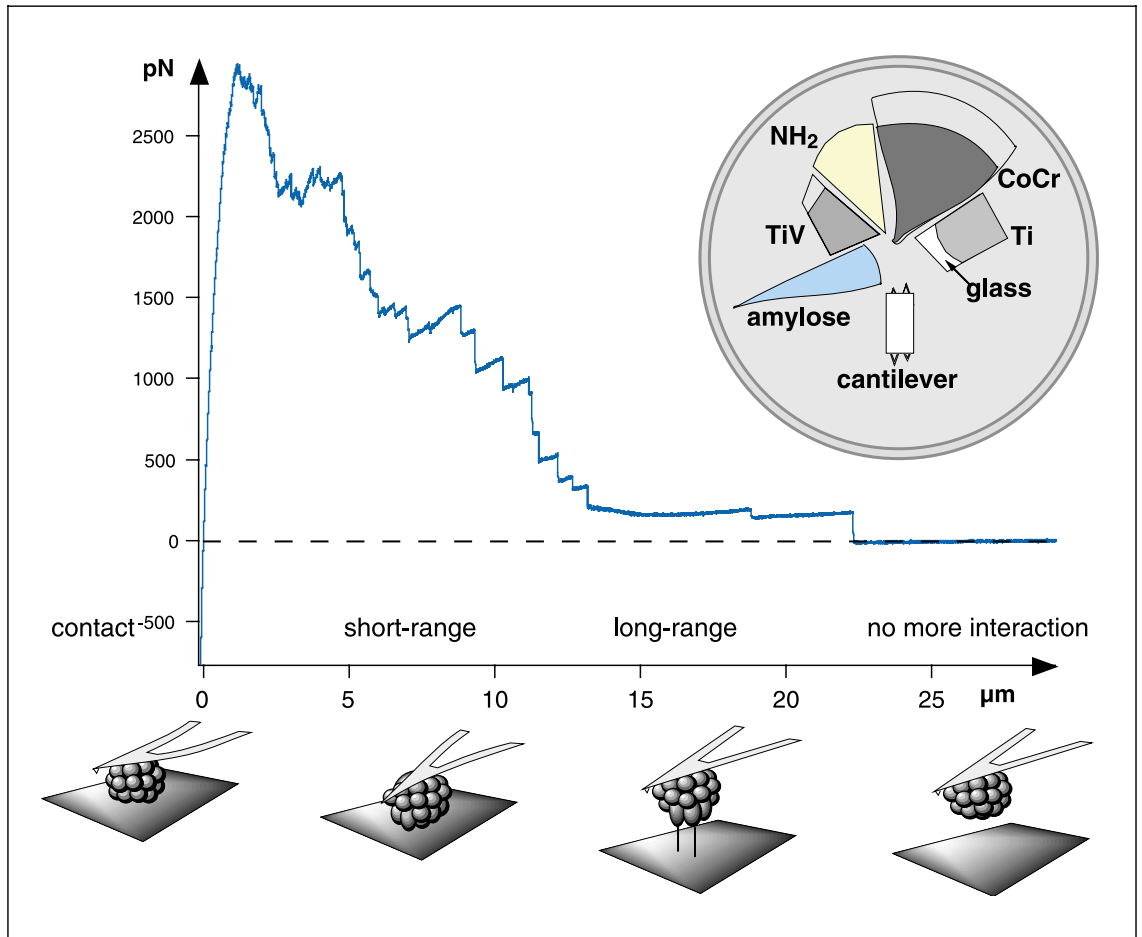
Fig. 5. Force-distance plot (blue) from an experiment with a bone cell layer on a sphere involving different surfaces arranged in a Petri dish (inset) and schematic illustration of the experiment (below). After the cell contact (negative contact force) the layer is stretched and the adhesion load increases until the maximum adhesion force (here 2.9 nN) is reached. On further separation the descending force pattern gets marked by individual force steps indicating molecular de-adhesion events. The steps after a flat plateau (e.g. the last three) show the typical signature for tether formation (long-range interaction).
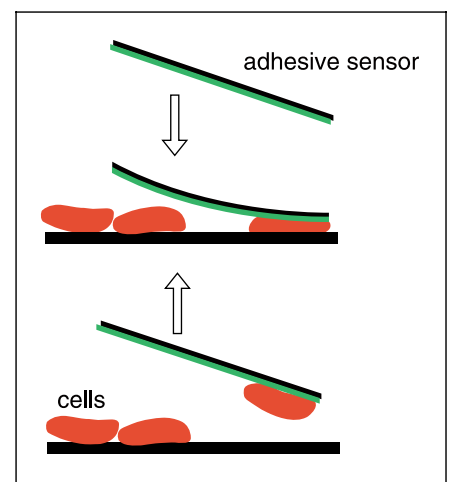

Fig. 6. 'Cell fishing'. With an adhesive sensor without tip a loosely attached cell is focussed on, held in contact at up to a few nanonewtons for some seconds and lifted up.

ization from confluent cultures, counted and adjusted to the desired concentration (2–3.5 × 10^5 and 1 × 10^5 cells/ml for RL95 and JAR cells, respectively). Subsequently, we poured cell suspensions onto poly-*D*-lysine-coated glass coverslips within 4-cm^2 wells. We grew these cells to confluent monolayers and transferred them into a Petri dish before using them in experiments.

Red Blood Cells

Red blood cells of group A and 0 were freshly extracted from suitable individuals, diluted in PBS and separated from the serum by three centrifugation steps at 10,000 rpm for 2 min (microcentrifuge, 4214 ALC international, Monzese, Italy) in PBS pH 7.4.

They were immobilized as monolayers on aminosilanized glass slides, or as individual cells on force sensors that are covalently functionalized with WGA lectin (Sigma) 'fished' from a glass substrate (fig. 6).

Dictyostelium Cell Culture

All mutants were derived from the *D. discoideum* AX2-214 strain, designated here as wild type. Mutant HG1287 was generated by E. Wallraff [Beug et al., 1973a]. In mutant HG1287, csA expression was eliminated by a combination of chemical and UV mutagenesis. In this mutant, not only the csA but also other genes may have been inactivated by this general mutagenesis. Cells were cultivated in nutrient medium as described [Malchow et al., 1972] in Petri dishes up to a density of 1 × 10^6 cells/ml. For transformants HTC1 [Barth et al., 1994], CPH [Beug et al., 1973a] and T10 [Faix et al., 1992], 20 µg/ml of the selection marker G418 was added to stabilize csA expression. Before we took measurements on these cells, we washed and resuspended them in 17 mM K/Na buffer, pH 6.0. We used the cells either immediately (as undeveloped cells) or after shaking for 6 h at 150 rpm (as developing cells). The temperature was 20°C.

For the measurements, cells were suspended in 17 mM K/Na-phosphate buffer, pH 6.0, and were spread on polystyrene Petri dishes of a diameter of 3.5 cm at a density of about 100 cells/mm^2. To chelate Ca^{2+}, we added 5 mM EDTA at pH 6.0 in the same buffer. To avoid scattering of the laser beam of the detection system, we removed nonadherent cells by gently rinsing the dish after 10 min.

Results

Cell Layer-Substrate Interaction

To illustrate the interaction of a cell layer with a substrate, we selected the two experimental setups shown in figure 1B and E.

Adhesion of a Cell Layer to Varied Substrates

Bone cells (SaOS2) were grown to confluence on the bead glued to the cantilever. This illustrates the approach shown in figure 1E to test cell layer-substrate interaction. The cells are moved near a Petri dish or to a glass surface. We used glass surfaces that were uncoated, coated with cobalt-chromium, titanium, titanium-vanadium or aminosilane, or functionalized with carboxyamylose (fig. 5). The experiment was designed to measure the adhesive-ness of the various surfaces in the Petri dish to the monolayer immobilized on the sphere, as schematized in the inset of figure 5. The layers were brought into contact at a contact force of 200 ± 100 pN with the surfaces for varied durations of time, from milliseconds to 10 min, either in HBSS or nutrient medium. From the force versus distance plots (like in the one in fig. 5), we obtained the maximum adhesion force.

For each surface, contact time and medium, we examined 8 or more force traces to compute the maximum adhesion forces. The amount of variance in the adhesion forces between different preparations and within the experiment's time turned out to be large. Thus the averages listed in table 1 are not too significant. The setup used to study the interactions between cell layer and surfaces (fig. 1E) is included despite the poor statistics. Nevertheless, these and other measurements (not shown) clearly indicate that the maximum adhesion force increases relative to the contact time until it eventually levels off. No differences were resolved between maximum adhesion forces after a contact with metal surfaces or pure glass or Petri dish surfaces of less than 1 s. The forces seem to be smaller in respect of amylose-functionalized surfaces and larger in respect of NH$_2$-functionalized surfaces. In nutrient medium, the maximum adhesion forces in respect of the different surfaces appear to be similar except that the adhesion forces obtained with the amylose surface tended to stay lowest while those achieved with the Petri dish were slightly higher. The enhanced maximum adhesion forces after 10 min of contact between the cell layer and the surface is markedly weaker in nutrient medium than in HBSS for all surfaces except that of the Petri dish (table 1). The difference between the adhesion to a glass surface and a metal surface might be enhanced in HBSS. The NH$_2$ surface showed the strongest adhesion in HBSS but also dropped close to 1 nN in nutrient media whereas with amylose it remained unchanged at about 1 nN. After 10-min contacts in nutrient medium all surfaces, including NH$_2$ and amylose, show the same reduced adhesion, the exception being the surface of the Petri dish.

The contact area between the interacting surfaces is approximated via light-microscopic observation as 140 ± 60 µm^2. The area of the surfaces in contact depends on the contact force and the elasticity and thickness of the layer of cells. The adhesion force increases relative to the contact area. This is one of the reasons for the variability of the measured maximum adhesion forces of this setup.

Instead of separating the cells completely while measuring the de-adhesion force, now the interacting cells

Table 1. Cell layer interaction with different surfaces

	Glass	CoCr	Ti	TiV	Petri dish	NH_2	Amylose
1 s							
HBSS, pN	92 ± 56	71 ± 41	95 ± 67	89 ± 57	89 ± 46	166 ± 68	38 ± 7
$SaSO_2$, pN	74 ± 60	60 ± 17	89 ± 37	60 ± 30	116 ± 55	127 ± 54	44 ± 5
10 min							
HBSS, nN	1.4 ± 0.5	1.9 ± 0.9	2.6 ± 1.7	3.2 ± 0.4	2.8 ± 1.6	6.1 ± 2.1	1.3 ± 0.6
$SaSO_2$, nN	0.8 ± 0.4	0.6 ± 0.3	0.8 ± 0.5	1.0 ± 0.3	4.3 ± 2.0	0.7 ± 0.1	1.0 ± 0.6

Each maximum adhesion force was averaged from only 8–20 measurements after contacts of 1 s (above) or 10 min (below) in $SaOS_2$ medium or in HBSS. A column represents the material of a surface brought in contact with the cell layer. Due to the high variability and the poor statistics the confidence interval is often large.

were only slightly elongated and released again after a certain period of time. Bond rupture, therefore, plays a minor role whereas elastic and viscous elements of the cell layer dominate the signal.

Viscoelastic Properties of Cell Layers

A sphere (diameter 60 μm) on the sensor was coated with fibronectin adhesive and brought into contact with a confluent epithelial cell layer (fig. 1D) for a period of time (e.g. 20 min) sufficient to establish strong adhesion. We then applied a mild pulling or indentation load that did not suffice to separate the sphere from the cells. In this experiment, we did not detect the adhesion force but rather the viscoelastic properties of the cell layer. We applied this square waved load to three types of cells (JAR, HEC, RL) (fig. 7). The resulting force versus time plot (fig. 7) can be described as follows: in response to an abrupt pulling for a few micrometers, the measured force increased rapidly, mimicking the response of a purely elastic load. When we arrested the elongating piezo element, the measured force decreased exponentially, resembling a spring in parallel with a dashpot. When we restored the original position, the detected force instantaneously dropped to negative values, indicating that the cells resist recompression. While arresting the piezo again, the viscous element crept back exponentially until this time a negative force was approximated. This measurement cycle could be repeated up to 30 times until the deviations from the initial circle caused by drift and slow but continued bond rupture or alteration of the cell structure as a result of pulling became significant. When comparing the effects of force relative to time to those of standard viscoelastic models, a creep function of the Maxwell body model corresponds best with our data. It consists of a spring parallel to a series of other springs and a dashpot. As depicted in figure 7 the viscoelastic elements of the cell layers were calculated from this model and are listed in table 2. We have to state that there was a large variability between different preparations in the measured values of the fairly soft JAR and HEC cell layers. Here plastic deformation of the cells causes large drift effects.

Single Cell Interaction

We selected the red blood cell for a more controlled adhesion experiment (fig. 1A). Moreover, we characterized the de-adhesion force of single csA-csA connections between live *D. discoideum* cells.

Immobilizing a Single Living Cell on a Force Sensor

As shown by Razatos et al. [Razatos et al., 1998] individual bacteria can be fixed to a cantilever. An appropriately functionalized force sensor is used to tether a living cell sitting loosely on a culture dish to the sensor. To this end, the lever is lowered onto the cell with a force of a few nano-newtons and is held in contact for approximately 30 s, to allow the molecules on the lever to bind, before the cell is lifted off the bottom of the dish (fig. 7). If the cell adheres to the sensor, it can be moved to a cell or surface of interest. Typically, the interaction strength between cell and cantilever increases with time, presumably due to the development of connections. Best results were obtained with tipless cantilevers, probably because the tip either interferes with the adhesion measurement if it surmounts the cell or because it hinders the cell adhesion. Unfortunately, commercial tipless cantilevers are very stiff (Digital Instruments, 60 mN/m) compared to the soft cells [Radmacher et al., 1996].

In order to obtain compliant and tipless force sensors the cantilevers had to be modified destructively with thin tweezers prior to functionalization (fig. 4). The tip of a
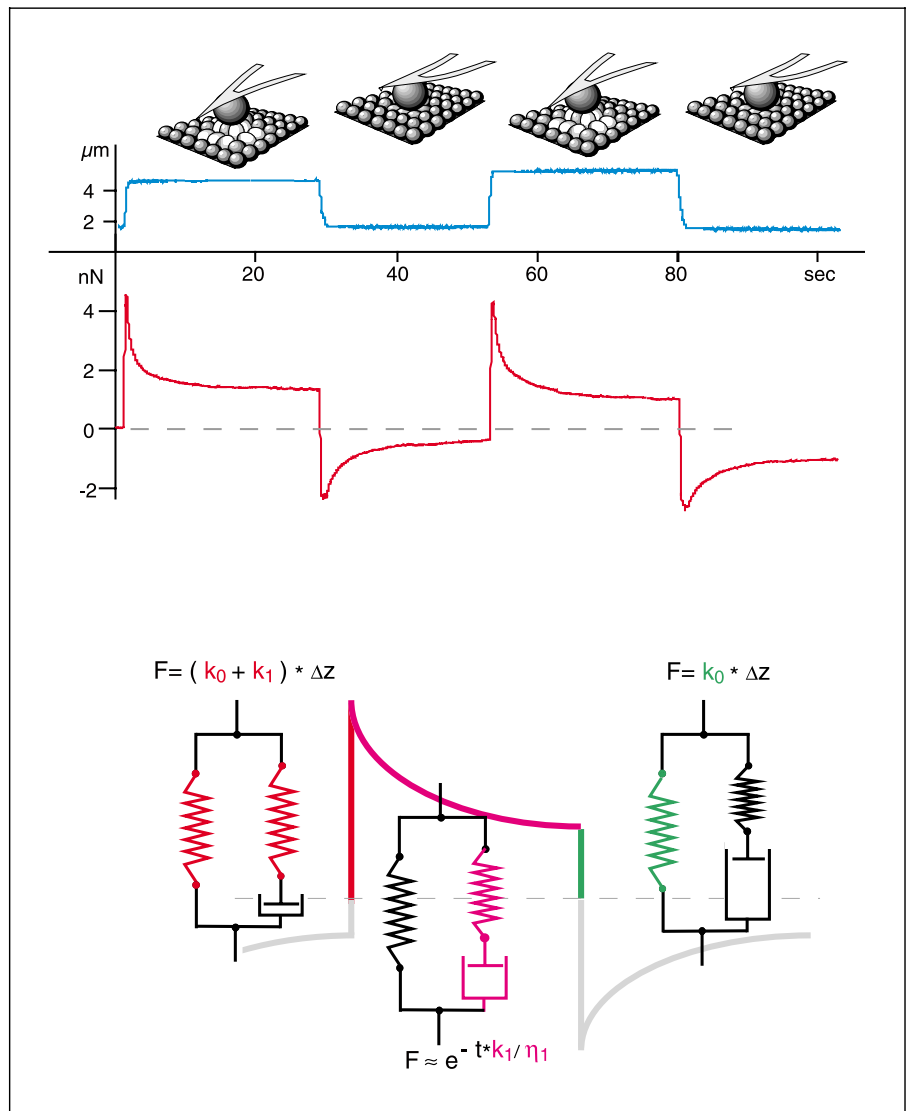
Fig. 7. The characteristic force pattern (creep function – red line) of a 'Maxwell body' arises when applying the rectangular load-relax pattern (blue line). Therefrom the viscous and elastic components of the model can be derived (schematics below): k_0 and k_1 from the initial stretching of both springs; k_1/η_1 by an exponential fit to the decreasing force; finally k_0 remains when the viscous element η_1 is elongated until k_1 is unloaded.

$$F = (k_0 + k_1) * \Delta z$$

$$F = k_0 * \Delta z$$

$$F \approx e^{-t*k_1/\eta_1}$$

soft cantilever was removed and the breaking off of one of the legs additionally reduced the spring constant by half.

Measurements on Red Blood Cells

In order to illustrate the interaction of single cells and to introduce general strategies for measuring single adhesion molecules on cell surfaces, we investigated an artificial adhesion between red blood cells in PBS solution. A target cell resting at the bottom of a Petri dish was positioned under the cell on the adhesive functionalized cantilever. We then moved one cell closer to the other until a predefined repulsive contact force was established (fig. 8). This contact force was held constant for a defined time interval in order to allow the cells to adhere to each other.

Table 2. Viscoelastic constituents of the Maxwell model

	k_0, nN/µm	k_1, nN/µm	η_1, nN/µm
JAR	0.7 ± 0.5	2.1 ± 1.1	25 ± 5.2
HEC	0.8 ± 0.6	1 ± 0.9	4.9 ± 3.8
RL	5.3 ± 0.4	3.5 ± 0.8	27 ± 4.7

Values for the viscoelastic elements (k = spring constant, η = viscous drag) of 3 different cell types (JAR, HEC and RL) are shown.
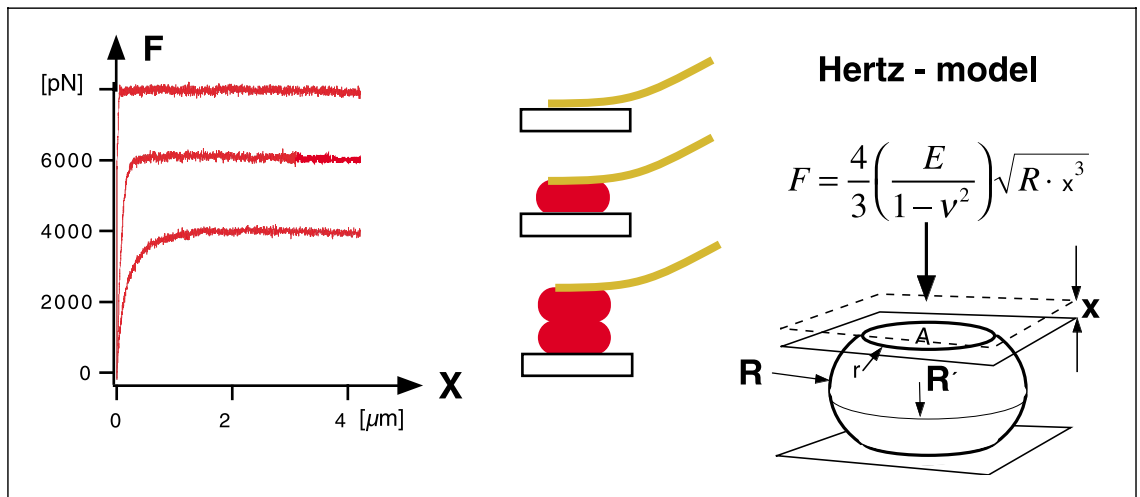
Fig. 8. Three different force curves from the approach phase (plotted from right: 4 μm to left: 0 μm) a plain sensor upon the plain substrate (above), a cell on the sensor upon the plain substrate (middle) and upon another cell (below). The sensor-deflecting force is repulsive during contact and stops the approach at a certain threshold (here 4 nN) in all three cases. The Youngs modulus E at a given Poisson ratio ν can be calculated with the Hertz model [Hertz, 1882] from the indentation x and the load F after measuring the radius R of the cell.

As shown in figure 8 elastic properties of the red cells can be measured in this geometry by applying the Hertz model [Domke and Radmacher, 1998]. Steeper slopes of the force-distance plots correlated with harder tested substrates. Red blood cells in vivo do not adhere at all (fig. 9A), presumably to sustain blood flow. Figure 9B shows adhesion induced by the addition of lectins (100 μg/ml; like WGA, Sigma) that bind to the surface-expressed glycosylated proteins.

In the last step traces of de-adhesion force could be observed with a pattern typical of tether formation: a flat plateau is followed by a step. Tethers are lipid bilayer membrane tubes pulled out of a vesicle or cell. These tethers resist expansion with a constant force that is independent of extension [Hochmuth et al., 1996].

Reducing the lectin concentration, the contact force or the contact time leads to force distance traces reflecting the weakest interaction (fig. 10A). The adhesion probability is decreased to less than 40% under those conditions and the probability of rupturing only single lectin bonds is in the order of 90%.

We present these small final rupture forces (n = 3,200) in a histogram (fig. 10B). This distribution indicates that 70 ± 5 pN is the most probable rupture force for a single WGA-glycocalyx complex. This is consistent with the data obtained when measuring the rupture force between

Helix pomatia lectin (HPL) that had been immobilized on a cantilever and red blood cells of group A [Grandbois et al., 2000] and which indicate that 65 ± 5 pN is the most probable de-adhesion force (fig. 10C).

In these simplified experiments, the stable red blood cells could not alter the results actively. Thus the influence of the contact time, contact force and concentration of the lectin molecules was identified and the measurement of single adhesion molecules on living cells could be attempted.

Measurements on *D. discoideum*

As described above, a *Dictyostelium* cell is picked up with a tipless AFM cantilever whose end had been covalently functionalized with WGA lectin (Sigma).

The adhesion of the nondeveloped cells used in this experiment is known to be Ca^{2+}-dependent [Beug et al., 1973b]. The Ca^{2+}-sensitive adhesion vanished when 5 mM of EDTA, a chelating agent, was added to the buffer. This low amount of EDTA did not affect the cells' integrity for the duration of the experiments. Since the cells tended to move along the surface of the dish it was necessary to monitor their contact with a built-in light microscope and readjust their positioning accordingly.

In the presence of 5 mM EDTA, 96% of the cells did not establish detectable adhesion within 0.2 s, even when

Fig. 9. The force curves obtained when separating two red blood cells show no adhesion (**A**); however, they show a significant adhesion (**B**), when lectin (WGA) is added to the medium (here an additional three consecutive force curves are superimposed). The almost linearly ascending beginning of the force curve in the low force regime indicates elastic behavior. Reaching the maximum adhesion force, most of the bonds rupture. Beyond this maximum the backbone of the cell is more or less disconnected from the interacting molecules. Finally all membrane elements (mainly tethers) refuse to maintain the contact while reaching the end of the curve.
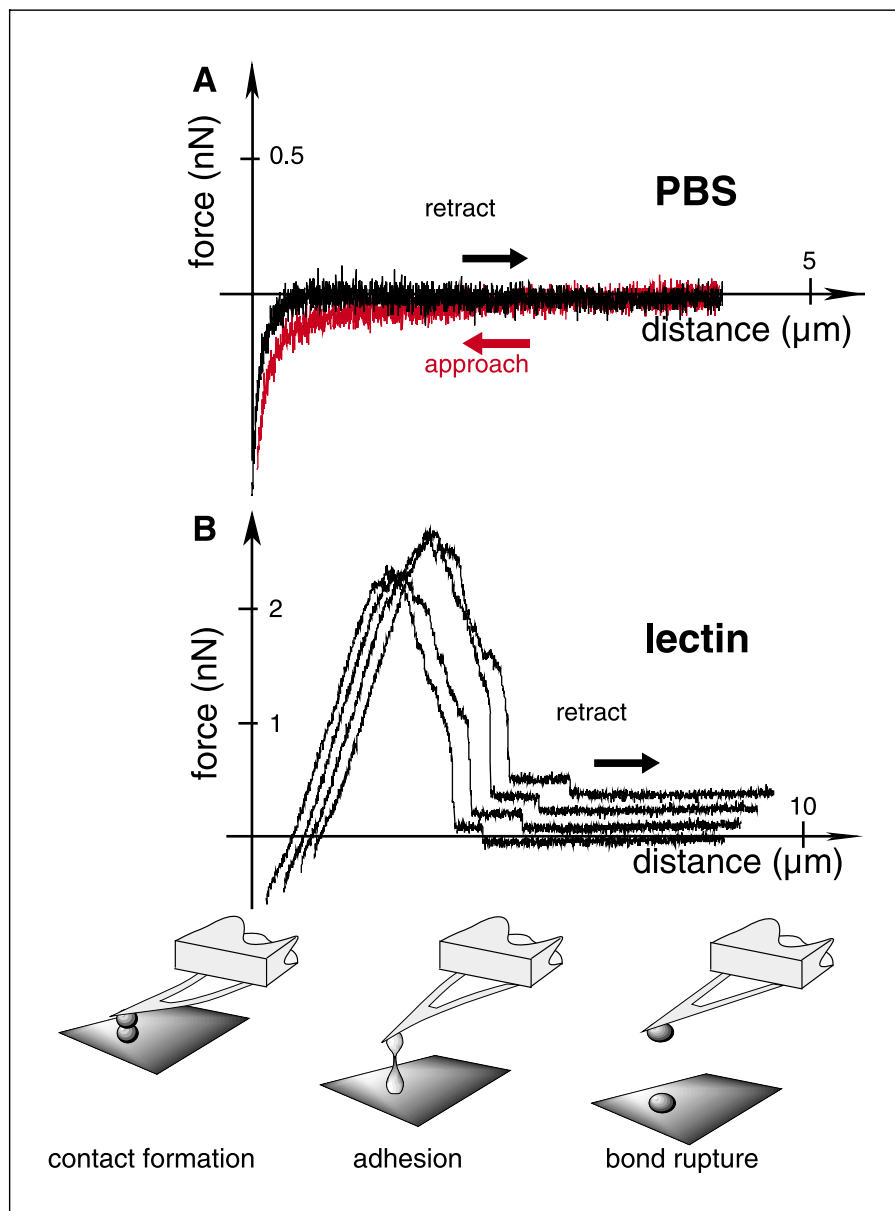
they were brought into contact using an increased force of 100 pN (fig. 11A). On the basis of these data de-adhesion forces were measured in developing cells in which additional cell adhesion proteins are expressed. Aggregating cells in the developing stage are distinguished from non-developing cells in the growth phase by EDTA-stable cell adhesion [Beug et al., 1973a]. When 5 mM EDTA was added to these cells and de-adhesion forces were determined after a contact force of 35 ± 5 pN, binding was observed in roughly half of the traces. The collection of traces shown in figure 11B illustrates the type of results

obtained at different contact times. Often initial forces rose up to several hundred pico-newtons and unbinding occurred in several steps until the last tether connecting the two cells at the location of long contacts was disrupted. In contrast to these multiple de-adhesion events, single steps of de-adhesion prevailed after a contact time of 0.2 s.

The last force step, the one that completely separated the cells, was measured in more than 1,000 traces after contact times of 2, 1 or 0.2 s (fig. 11). When these data were compiled in histograms, a pronounced peak, indicat-

ing a force quantum of 21 ± 5 pN, became apparent. Upon increasing contact times from 0.2 to 2 s, this peak shifted only negligibly in the direction of higher de-adhesion forces (23 pN). The main difference between the histograms resided in the lower contribution of higher forces upon the reduction of contact time. The higher forces contributing to de-adhesion after 2 or 1 s of cell-to-cell contact can be interpreted as superimposed multiples of a basic force quantum of 23 pN.

Developmental regulation and EDTA resistance suggest that the measured force quantum of 23 pN is due to the unbinding of csA molecules. However, cells in the aggregation stage differ from growth phase cells not only in the csA protein but also in several other developmentally regulated cell surface proteins. Therefore, in order to attribute the peak of 23 pN to the presence of this particular cell adhesion protein, different types of cells in which specifically csA expression was genetically manipulated were employed [Benoit et al., 2000]. The csA gene was selectively inactivated by targeted disruption using a transformation vector that recombined into the gene's coding region [Faix et al., 1992] (fig. 12A). Only 25% of the cells in this csA knockout strain showed measurable de-adhesion forces.
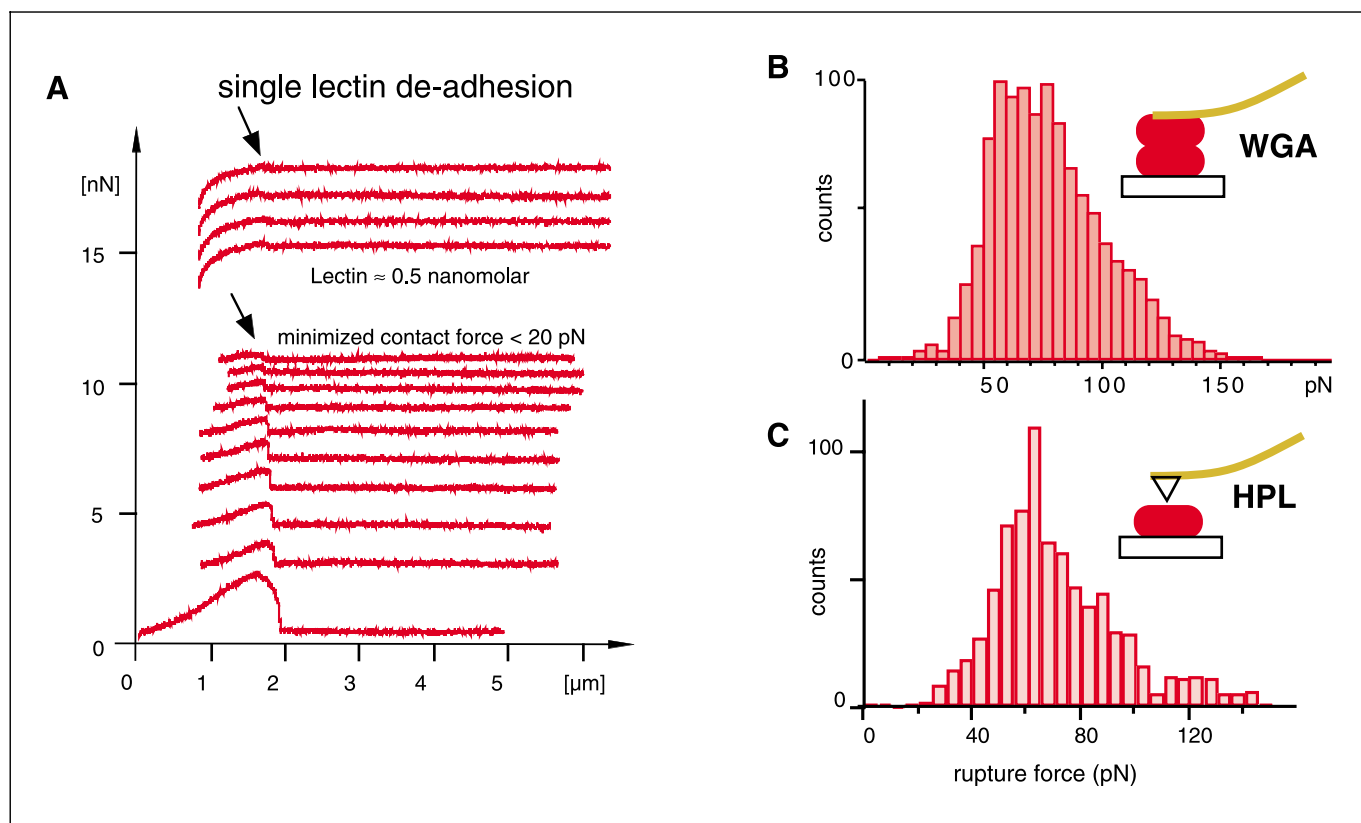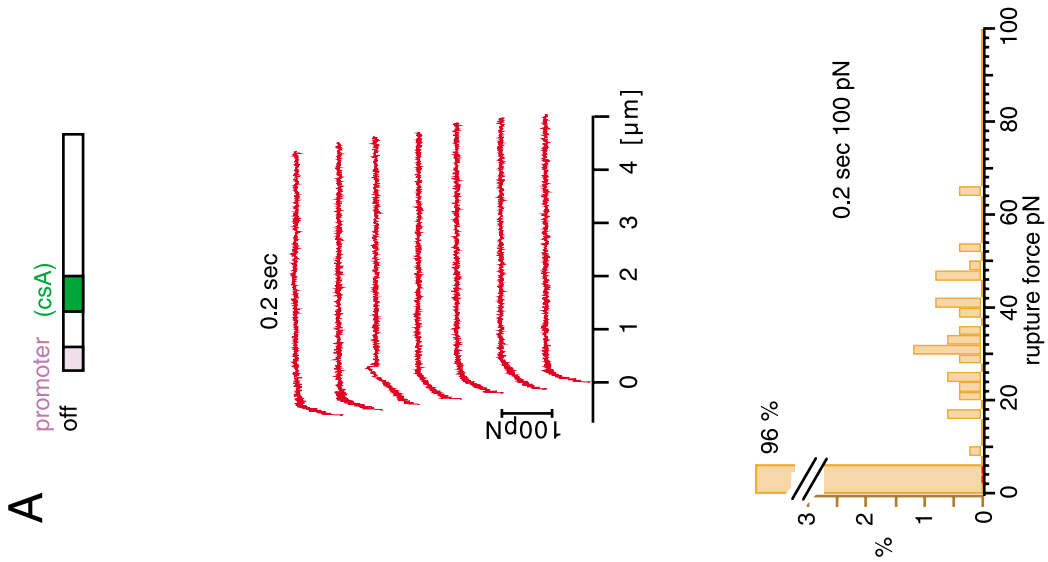

Fig. 10. A Adhesion between single lectin molecules is achieved by either a low lectin concentration (0.5 nM) at 500 pN contact force (first 4 curves) or minimized contact force and contact time at a higher concentration (0.1 μM). **B** A histogram of the last rupture force of each force curve measured at shortest contact times (0.2 s) and weakest contact forces (a few pN) between red blood cells in lectin solution (0.1 μM) collected from 3,200 traces. The most probable de-adhesion force is 70 ± 5 pN. **C** A histogram of the last de-adhesion forces between a cantilever covalently functionalized with lectin (HPL) and a red blood cell collected from 3,025 traces. The most probable de-adhesion force is 65 ± 5 pN.

Fig. 11. *D. discoideum* (wild-type) cell adhesion properties compared between starved (developing phase; **B**) and not starved (growth phase; **A**) cells. **A** The histogram of interacting growth phase cells was collected from the last rupture force of curves after contacts of 0.2 s at 100 pN as shown above. **B** The histograms of interacting cells with an active development promoter for contacts of 2, 1 and 0.2 s at 40 pN were obtained from the last rupture force (arrows) of curves as shown on the side. The most probable adhesion force for shortest contacts (0.2 s) is 23 ± 5 pN, the longer contact (1 and 2 s) contributions of multiple csA interactions enhance the histograms at twice and triple the force of 23 pN. Each histogram consists of at least 1,000 force measurements.
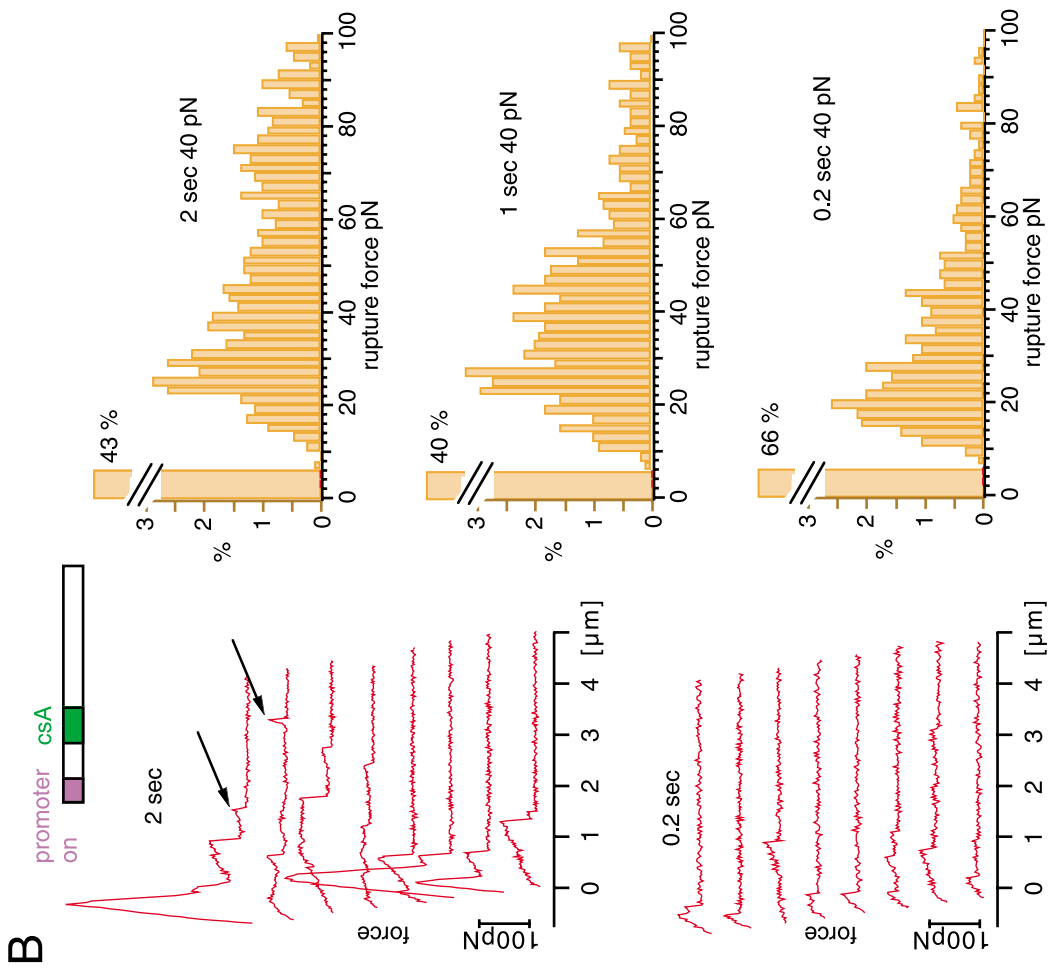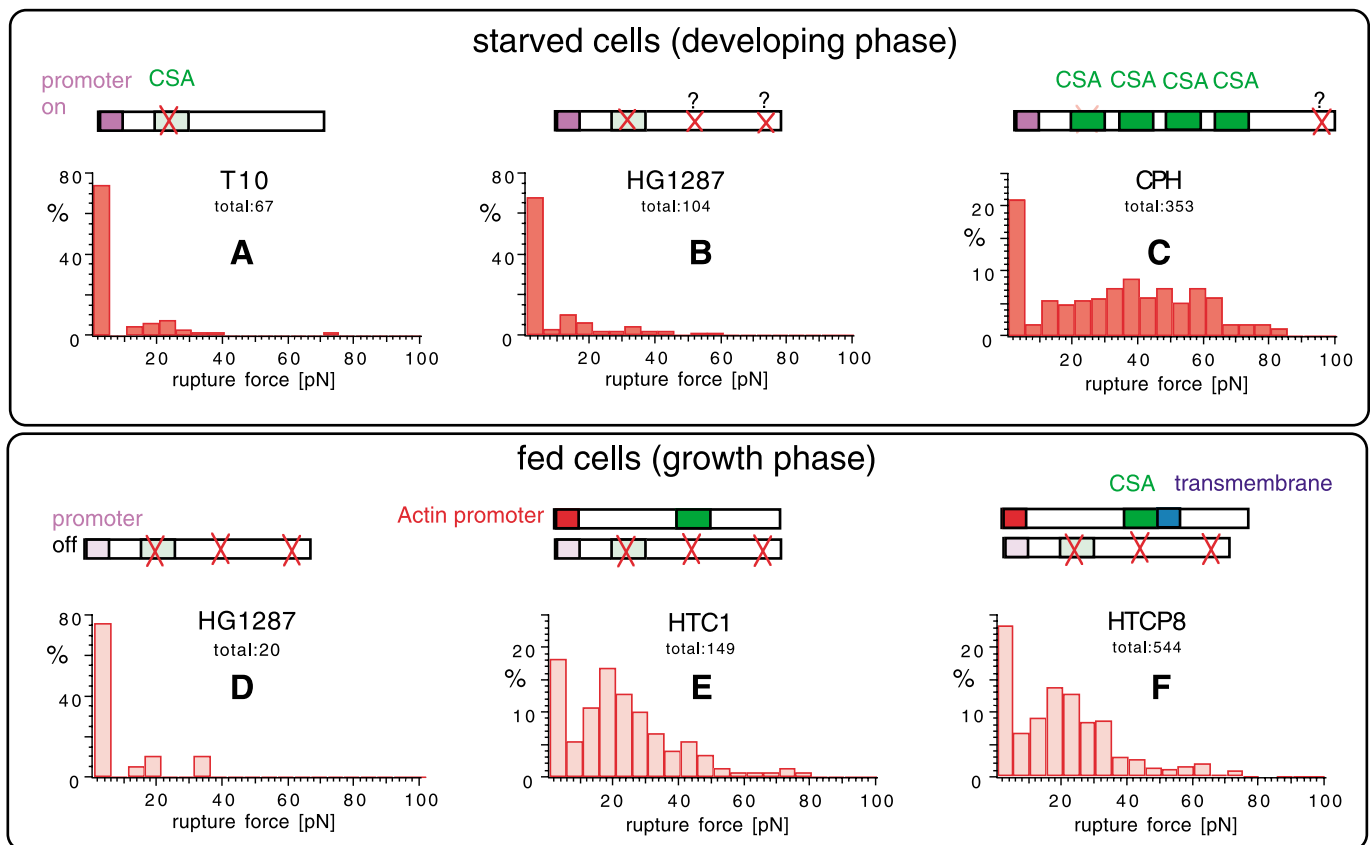
Fig. 12. Histograms of different mutants demonstrating the correlation between measured adhesion and expression of csA after contacts of 0.2 s at 150 pN. **A** Starved csA null mutant by point mutation (no adhesion). **B** Starved csA null mutant by gene disruption with possible additional genetic defects '?' (no adhesion). **C** Starved mutant (**B**) with multiple reinserted csA-coding regions (enhanced adhesion). **D** Mutant (**B**) in the growth phase (no adhesion). **E** Mutant (**B**) in the growth phase with a reinserted csA-coding region behind the actin 15 promotor (adhesion). **F** Mutant (**E**) in the growth phase encoding a transmembrane-anchored csA replacing the ceramid-anchored csA (adhesion).

Also, cells of a mutant that was unable to produce csA [Harloff et al., 1989] (fig. 12B, D) were transfected with vectors that encode the csA protein under the control of the original promoter. Indeed, these 'repaired' cells showed adhesion (fig. 12C) only when developing like the wild type. Another mutant 'repaired in a special way' produces a csA reading from a coding region that is switched by the actin promoter. These cells produce csA and show a histogram typical for csA adhesion despite not having been starved (fig. 12E).

Together these results demonstrate that the csA molecule is the primary source of the intercellular adhesion measured by force spectroscopy in the presence of EDTA. Finally, a mutant replacing the membrane anchor by a transmembrane anchor (fig. 12F) was employed to study the location of the bond rupture. Since the histogram does not differ significantly from the comparable histograms for csA-expressing cells, the anchorage of the molecule is obviously not involved in the de-adhesion process.

Discussion

Immobilization

The fact that the living cells have to be immobilized in order to measure forces with this technique might generate several alterations in the cells. Since several adhesion-induced intracellular rearrangement processes are known, the adhesive molecules that attach the cells should be selected carefully with respect to e.g. signaling effects. On the other hand, it is precisely those effects that can be detected with this technique. Furthermore, immo-

bilized cells, especially epithelial cells, polarize when immobilized and epithelial cell interaction is measurable with this setup [Thie et al., 1998]. Hence the measurements of the adhesion of various materials on the bone cell's apical surface presented here (fig. 5) are not directly comparable to cells seeded on these materials [Domke et al., 2000] and which establish contact with the basal membrane.

Loading Rate

Bond rupture experiments were performed under non-equilibrium conditions, and the measured forces are, therefore, rate-dependent. For this reason and so that they can be compared with each other, all experiments were performed at the same velocity. As shown by several groups [Grubmüller et al., 1995; Rief et al., 1998; Evans and Ludwig, 1999; Merkel et al., 1999], this rate dependence may reveal additional information about the binding potential. For living cells this detailed analysis is important in establishing the relationship between cell adhesion and the rate of cell movement or shear forces in the bloodstream [Chen and Springer, 1999]. The bone cells were separated at 7 μm/s from the substrates. For *Dictyostelium* and red blood cell experiments the separation rate was kept constant at 2.5 μm/s, resulting in force ramps between 50 and 500 pN/s, depending on the elasticity of the cells. Especially in the case of tethers, the loading rate is almost zeroed prior to the rupture.

Surface Area

Determining the characteristics of the adherent cell surface areas especially with long contact times is difficult. Obviously it is dependent on the contact force, but the contact time is also important for two uncontrollable reasons. First, the cells adapt their surfaces to each other and increase the area. Second, the drift of the instrument either enlarges or decreases the contact force with time. Due to these drift effects of the force detection system the duration of controlled contact between cells is limited to a few minutes. This means that many questions about long-time adhesion properties cannot be addressed by direct measurement with the force spectrometer.

The variability of the maximum adhesion force of different spheres measured on cell layers can therefore be as much as 100%, since the cell surfaces adapt to the substrate topography in a different way for each prepared sphere. An estimation of the density of adhesion molecules on the interacting cells is, therefore, not precise, but collective molecular changes become apparent with increasing contact time [Thie et al., 1998].

Surface Alteration

Sometimes the cell's shape alters during the measurement, e.g. due to pH shift or stress while measuring. Especially after strong adhesion, as was the case with NH_2 surfaces, parts of the membrane remained on the substrate. It cannot be ruled out that the cell surface is also altered destructively (e.g. the amount of adhesion molecules) when the surfaces are separated during the measurements. Therefore the cells were brought into contact with the different substrates in alternating order and perturbed the material of the first contact as well and experiments did not exceed 3 h. The strategy of the shortest contact time and the smallest contact force reduces all the problems associated with the interacting surfaces to a minimum, as shown with single cells. Furthermore, more experiments with short contacts, can be performed within a given time frame, which provides more robust statistics compared to experiments after long cell contacts. However, molecular processes like clustering or focal adhesion will no longer be detectable when this strategy is used.

Medium

The latest results in tissue engineering [Minuth et al., 2000] relate the behavior of cell differentiation to the influence of the ingredients of the nutrient medium and the substrate. The results presented here show the influence of the medium on the adhesion. Whereas the dependency on calcium is obviously related to the cells and adhesion molecules, in the case of the bone cell study the medium may also have altered the tested surfaces by unspecific contamination. The enhanced adhesion to Petri dishes (probably coated with collagens), optimized for cell culture in a nutrient medium, might be related to the conditions which are more favorable for the cells. But it is more likely that the molecules of the serum cover the charged NH_2 groups and passivate them. Similarly the metal and glass surfaces seem to be contaminated unspecifically and are leveled out. In this experiment, it is unknown which molecules mediated the adhesion. Nevertheless the original aim of the investigation with the bone cells on the sphere, which was to establish what the best surfaces for implants were, was not achieved using this approach: first, the metal surfaces did not show any drastic influence on bone cell adhesion after short contacts and contacts of 10 min. Second, in order to investigate acceptance, possible differences in the adhesiveness to the cells after days, or even months and years, are of interest. In the latter respect the surface roughness seems to play a dominant role [Domke et al., 2000].

This technique is not applicable when determining the long-term acceptance and adhesion of these materials as mentioned above. Due to intrinsic drift effects, the instrumental limitations at the time were contact times up to 1 h. In this regime the molecular arrangements that occur while establishing adhesive contacts between cells and surfaces become more prominent [Thie et al., 1998].

Cells

Living cells conceal the largest number of uncertainties in force spectroscopy experiments. They steadily undergo cell cycles and react to each other or to external stimuli. Especially in motile cells the cytoplasm changes its mechanical properties within minutes. The expression of adhesion molecules is induced from inside the cell or by signals from outside (e.g. starving *Dictyostelium*). Cells with a high potential surface to volume ratio (especially neurons) have so far not been amenable for this technique, since these cells tend to pull tethers strongly up to several millimeters [Dai and Sheetz, 1995] before separating. The z-range of our force spectrometer (maximum 100 μm) is consequently too small to measure their separation forces. Blood cells are relatively inert, lacking nucleus and adhesion molecules, and were therefore selected for preliminary experiments. Transformed blood cells expressing particular adhesion molecules would be a nice model system to pursue. *Dictyostelium* also turned out to be convenient because of its ability to switch the csA molecule and also because of the existence of many mutants.

Single Molecules

Even force-distance plots from de-adhesion measurements between cell layers reveal single de-adhesion events in the order of molecular interaction forces (fig. 5) [Thie et al., 1998]. The heights of these small de-adhesion steps obviously do not represent the molecular rupture force correctly except for the very last one, since other linkages between the cells can diminish each force step. However, focussing on the last de-adhesion step and reducing contact force and contact time not only isolates the direct force measurements obtained from single interacting pairs of molecules but also makes it possible to disregard the contact area. The quantized de-adhesion force of 23 pN from the *Dictyostelium* experiments indicates discrete molecular entities as the unit of csA-mediated cell adhesion (fig. 11). The most likely interpretation of this peak is that one unit reflects the interaction of two csA molecules, one on each cell surface. Nevertheless, since oligomerization may strongly increase the affinity of cell adhesion molecules [Tomschy et al., 1996], we cannot exclude the possibility that defined dimers or oligomers represent the functional unit of csA interactions [Baumgartner et al., 2000; Chen and Moy, 2000]. The histogram of prolonged contacts of up to 2 s (fig. 11) or of the mutant (fig. 12C), with the 'repaired' coding region reading multiple csA sequences, show a significant contribution of higher forces which can be explained by the higher probability of oligo-formation.

The measured de-adhesion force of 23 pN for csA is small compared to most antibody-antigen or lectin-sugar interactions, which frequently exceed 50 pN at comparable rupture rates [Dettmann et al., 2000]. In view of the limited force that the lipid anchor may withstand, much higher molecular unbinding forces would offer no advantage.

Outlook

The combination of nanophysics with cell biology establishes a mechanical assay that relates qualitatively cooperative molecular processes during contact formation, or even quantitatively the expression of a gene, to the function of its product in cell adhesion. This type of single-molecule force spectroscopy performed on live cells is directly applicable to a variety of different cell adhesion systems. A wide field of application for this cell-based molecular assay is predictable, for instance when investigating mutated cell adhesion proteins or the coupling of cell adhesion molecules to the cytoskeleton and also when evaluating adhesion-blocking drugs. Individual cells in mixed tissue samples could be distinguished and isolated for further culturing [Grandbois et al., 2000]. Furthermore, initial steps in the receptor-mediated adhesion of particles to phagocyte surfaces can be measured with this technique and the interaction of cells with natural and artificial surfaces will also be of medical interest.

References

Alon, R., D.A. Hammer, T.A. Springer (1995) Lifetime of the P-selectin-carbohydrate bond and its response to tensile force in hydrodynamic flow. Nature *374:* 539–542.

Barth, A., A. Müller-Taubenberger, P. Taranto, G. Gerisch (1994) Replacement of the phospholipid-anchor in the contact site A glycoprotein of *Dictyostelium discoideum* by a transmembrane region does not impede cell adhesion but reduces residence time on the cell surface. J Cell Biol *124:* 205–215.

Baumgartner, W., P. Hinterdorfer, W. Ness, A. Raab, D. Vestweber, H. Schindler, D. Drenckhahn (2000) Cadherin interaction probed by atomic force microscopy. Proc Natl Acad Sci USA *97:* 4005–4010.

Benoit, M., D. Gabriel, G. Gerisch, H.E. Gaub (2000) Discrete molecular interactions in cell adhesion measured by force spectroscopy. Nat Cell Biol *2:* 313–317.

Beug, H., F.E. Katz, G. Gerisch (1973a) Dynamics of antigenic membrane sites relating to cell aggregation in *Dictyostelium discoideum.* J Cell Biol *56:* 647–688.

Beug, H., F.E. Katz, A. Stein, G. Gerisch (1973b) Quantitation of membrane sites in aggregating Dictyostelium cells by use of tritiated univalent antibody. Proc Natl Acad Sci USA *70:* 3150–3154.

Binnig, G., C.F. Quate, C. Gerber (1986) Atomic force microscope. Phys Rev Lett *56:* 930–933.

Chen, A., V.T. Moy (2000) Cross-linking of cell surface receptors enhances cooperativity of molecular adhesion. Biophys J *78:* 2814–2833.

Chen, S., T.A. Springer (1999) An automatic breaking system that stabilizes leukocyte rolling by an increase in selectin bond number with shear. J Cell Biol *144:* 185–200.

Clausen-Schaumann, H., M. Seitz, R. Krautbauer, H. Gaub (2000) Force spectroscopy with single bio-molecules. Curr Opin Chem Biol *4:* 524–530.

Dai, J., M.P. Sheetz (1995) Mechanical properties of neuronal growth cone membranes studied by tether formation with optical tweezers. Biophys J *68:* 988–996.

Dettmann, W., M. Grandbois, S. Andrè, M. Benoit, A.K. Wehle, H. Kaltner, H.-J. Gabius, H.E. Gaub (2000) Differences in zero-force and force-driven kinetics of ligand dissociation from β-galactoside-specific proteins (plant and animal lectins, immunoglobulin G) monitored by plasmon resonance and dynamic single molecule force spectroscopy. Arch Biochem Biophys *338:* 157–170.

Domke, J., S. Dannöhl, W.J. Parak, O. Müller, W.K. Aicher, M. Radmacher (2000) Substrate dependent differences in morphology and elasticity of living osteoblasts investigated by atomic force microscopy. Colloids Surf B Biointerfaces *19:* 367–379.

Domke, J., M. Radmacher (1998) Measuring the elastic properties of thin polymer films with the atomic force microscope. Langmuir *14:* 3320–3325.

Evans, E., F. Ludwig (1999) Dynamic strength of molecular anchoring and material cohesion in fluid biomembranes. J Phys Condens Matter *11:* 1–6.

Evans, E., R. Merkel, K, Ritchie, S. Tha, A. Zilker (1994) Picoforce method to probe submicroscopic actions in biomembrane adhesion; in Bongrand P., A. Curtis (eds): Methods for Studying Cell Adhesion. Berlin, Springer.

Faix, J., G. Gerisch, A.A. Noegel (1992) Overexpression of the csA cell adhesion molecule under its own cAMP-regulated promoter impairs morphogenesis in *Dictyostelium.* J Cell Sci *102:* 203–214.

Florin, E.L., M. Rief, H. Lehmann, M. Ludwig, C. Dornmair, V.T. Moy, H.E. Gaub (1995) Sensing specific molecular interactions with the atomic force microscope. Biosens Bioelectron *10:* 895–901.

Gaub, H.E., J.M. Fernandez (1998) The molecular elasticity of individual proteins studied by AFM-related techniques. AvH-Magazin *71:* 11–18.

Grandbois, M., W. Dettmann, M. Benoit, H.E. Gaub (2000) Affinity imaging of red blood cells using an atomic force microscope. J Histochem Cytochem *48:* 719–724.

Grubmüller, H., B. Heymann, P. Tavan (1995) Ligand binding: Molecular mechanics calculation of the streptavidin-biotin rupture force. Science *271:* 997–999.

Harloff, C., G. Gerisch, A.A. Noegel (1989) Selective elimination of the contact site A protein of *Dictyostelium discoideum* by gene disruption. Genes Dev *3:* 2011–2019.

Hertz, H. (1882) Über die Berührung fester elastischer Körper. J Reine Angew Mathematik *92:* 156–171.

Hochmuth, R.M., J.-Y. Shao, J. Dai, M.P. Sheetz (1996) Deformation and flow of membrane into tethers extracted from neuronal growth cones. Biophys J *70:* 358–369.

John, N., M. Linke, H.-W. Denker (1993) Quantitation of human choriocarcinoma spheroid attachment to uterine epithelial cell monolayers. In Vitro Cell Dev Biol *29A:* 461–468.

Kuo, S.C., D.A. Hammer, D.A. Lauffenburger (1997) Simulation of detachment of specifically bound particles from surfaces by shear flow. Biophys J *73:* 517–531.

Kuramoto, H., S. Tamura, Y. Notake (1972) Establishment of a cell line of human endometrial adenocarcinoma in vitro. Am J Obstet Gynecol *114:* 1012–1019.

Malchow, D., B. Nägele, H. Schwarz, G. Gerisch (1972) Membrane-bound cyclic AMP phosphodiesterase in chemotactically responding cells of *Dictyostelium discoideum.* Eur J Biochem *28:* 136–142.

Merkel, R., P. Nassoy, A. Leung, K. Ritchie, E. Evans (1999) Energy landscapes of receptor-ligand bonds explored with dynamic force spectroscopy. Nature *397:* 50–53.

Minuth, W.W., K. Schumacher, R. Strehl, S. Kloth, (2000) Physiological and cell biological aspects of perfusion culture technique employed to generate differentiated tissues for long term biomaterial testing and tissue engineering. J Biomaterials Sci Polymer *11:* 495–522.

Patillo, R.A., A. Ruckert, R. Hussa, R. Bernstein, E. Delfs (1971) The JAR cell line – continuous human multihormone production and controls. In Vitro *6:* 398.

Radmacher, M., M. Fritz, C.M. Kacher, J.P. Cleveland, P.K. Hansma (1996) Measuring the visco-elastic properties of human platelets with the atomic force microscope. Biophys J *70:* 556–567.

Razatos, A., Y.-L. Ong, M.M. Sharma, G. Georgiou (1998) Molecular determinants of bacterial adhesion monitored by AFM. Proc Natl Acad Sci USA *95:* 11059–11064.

Rief, M., J.M. Fernandez, H.E. Gaub (1998) Elastically coupled two-level systems as a model for biopolymer extensibility. Phys Rev Lett *81:* 4764–4767.

Scott, G., H. Liang, L. Cassidy (1995) Developmental regulation of focal contact protein expression in human melanocytes. Pigment Cell Res *4:* 221–228.

Thie, M., B. Harrach-Ruprecht, H. Sauer, P. Fuchs, A. Albers, H.-W. Denker (1995) Cell adhesion to the apical pole of epithelium: A function of cell polarity. Eur J Cell Biol *66:* 180–191.

Thie, M., R. Röspel, W. Dettmann, M. Benoit, M. Ludwig, H.E. Gaub, H.-W. Denker (1998) Interactions between trophoblast and uterine epithelium: Monitoring of adhesive forces. Hum Reprod *13:* 3211–3219.

Tomschy, A., C. Fauser, R. Landwehr, J. Engel (1996) Homophilic adhesion of E-cadherin occurs by a co-operative two-step interaction of N-terminal domains. EMBO J *15:* 3507–3514.

Way, D.L., D.S. Grosso, J.R. Davis, E.A. Surwit, C.D. Christian (1983) Characterization of a new human endometrial carcinoma (RL95-2) established in tissue culture. In Vitro *19:* 147–158.

Zahalak, G.I., W.B. McConnaughey, E.L. Elson (1990) Determination of cellular mechanical properties by cell poking, with an application to leukocytes. J Biomech Eng *112:* 283–294.